Numerical Calculation of the Dielectric Spectra and Electrorotation Velocity of Cells

Viviana Zimmerman[a], Constantino Grosse[a,b]
Vladimir N. Shilov[c]

a - Departamento de Física, Universidad Nacional de Tucumán, Tucumán, Argentina. e-mail: vzimmerman@herrera.unt.edu.ar

b - CONICET, Argentina.

c - Institute of Biocolloid Chemistry, National Academy of Sciences, Kiev, Ukraine.

Introduction

Numerical methods have been widely used to study the dielectric and electrokinetic properties of colloidal suspensions of latex and soft particles (O'Brien and White, 1978; DeLacey and White, 1981; Mangelsdorf and White, 1992; Mangelsdorf and White, 1997; López-García et al., 2000; Saville, 2000; López-García and Horno, 2002). However, this methods were only very recently used for suspensions of cell-type particles (Zimmerman et al., 2003; Zimmerman and Grosse, 2004).

In this work, the network simulation method (López-García and Horno, 2002) is used to solve the electric potential, ion number concentration, and fluid velocity distributions induced by an AC electric field applied to a cell-type particle suspended in an electrolyte solution. Using the results, the induced dynamic dipole coefficient, dielectric spectra, and electrorotation spectra are calculated.

Cell model

- conducting internal medium
- non-conducting membrane
- external conducting layer: cell wall with an uniformly distributed fixed charge
- conducting external medium: electrolyte solution
- interfaces at R_b and R_c impermeable to the ions
- interface at R_a totally permeable to the ions

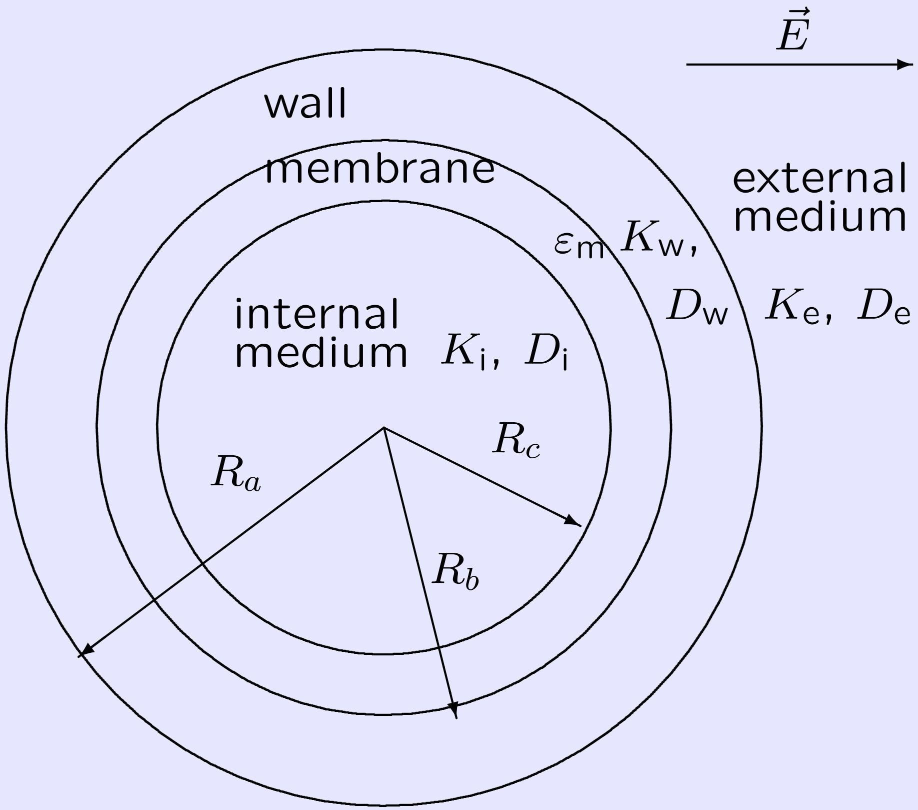

- only two type of ions are considered for every conductive medium
- the interface at R_a is permeable $\rightarrow$ the wall and the external medium are in equilibrium
- the wall and external medium permittivities are assumed to be identical (avoids the calculation of the Born energy term in the Poisson equation (Born, 1920))
- the hydrodynamic permeability of the wall is sufficiently low to impede liquid flow in this region (however, the ions can move inside the wall)
- the viscosity in the internal medium is high enough to impede the liquid flow, due to a possible inner cell structure

Dynamic dipole coefficient

The dynamic dipole coefficient (γ^*) is obtained solving the system with an applied *AC electric field*

$$\gamma^* = \lim_{r \to \infty} \left[\frac{r^2}{R_a^3 E_{\mathrm{o}}(t)} \left(\delta\phi(r,\, t) + E_{\mathrm{o}}(t) r \right) \right]$$

- the spectra obtained show the following dispersion regions:
  - α (related to the charge of the particle)
  - β (related to the process of charge of the membrane)
  - δ (Maxwell-Wagner-O'Konski dispersion)
- it was verified that the low frequency behaviour does not depend neither on the membrane thickness nor on the ion concentration in the internal medium for constant charge
- comparison between numerical and analytical results:
  - δ: very good coincidence
  - β: difference possibly due to the presence of charge; the difference increases when $\kappa_{\mathrm{e}} R_a$ diminishes
  - α: there are no-analytical predictions for the system considered

❖ *Spectra of the real part of the dipole coefficient for cells:*

∗ full lines: numerical

∗ dashed lines: analytical (uncharged particles)

(Zimmerman and Grosse, 2002)

$\kappa_e R_a = 10$

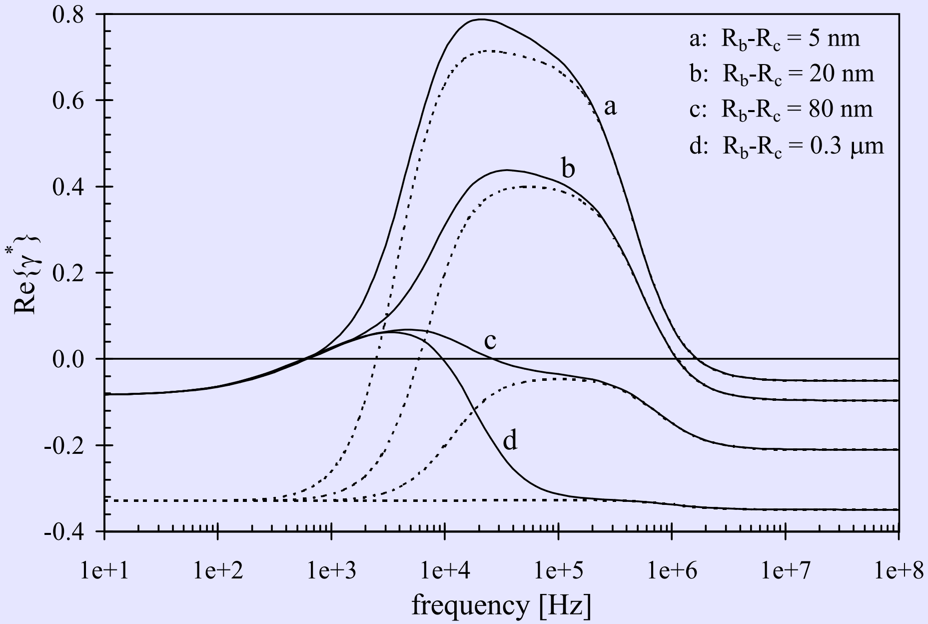

$\kappa_e R_a = 3$

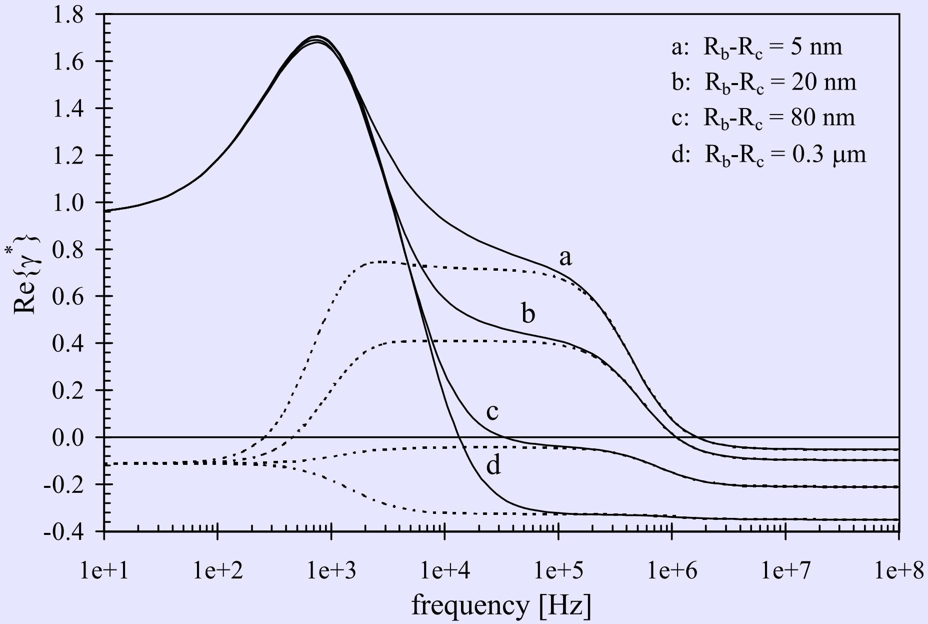

parameters used in the Figures

$R_a = 1.5\mu$m $\varepsilon_{\mathrm{e}} = 78.36$ $\varepsilon_{\mathrm{m}} = 4$ $\varepsilon_{\mathrm{i}} = 70$	$z_{\mathrm{e}}^{\pm} = z_{\mathrm{i}}^{\pm} = \pm 1$ $D_{\mathrm{e}}^{\pm} = D_{\mathrm{w}}^{\pm} = D_{\mathrm{i}}^{\pm} =$ 2×10^{-9} m^2/s $z^{\mathrm{f}} = -1$ $C^{\mathrm{f}} = 10^{23}$ 1/m^3 $\sigma_{\mathrm{i}} = 5\times 10^{-3}$ S/m	$\rho^{\mathrm{m}} = 10^3$ kg/m^3 $\rho^{\mathrm{p}} = 1.2\times 10^3$ kg/m^3 $\eta = 8.904\times 10^{-4}$ Pa s $T = 298.4$ K $R_a - R_b = 50$ nm	$\mathrm{N_e} = 300$ $\mathrm{N_w} = 300$ $\mathrm{N_i} = 200$ (number of compartments)

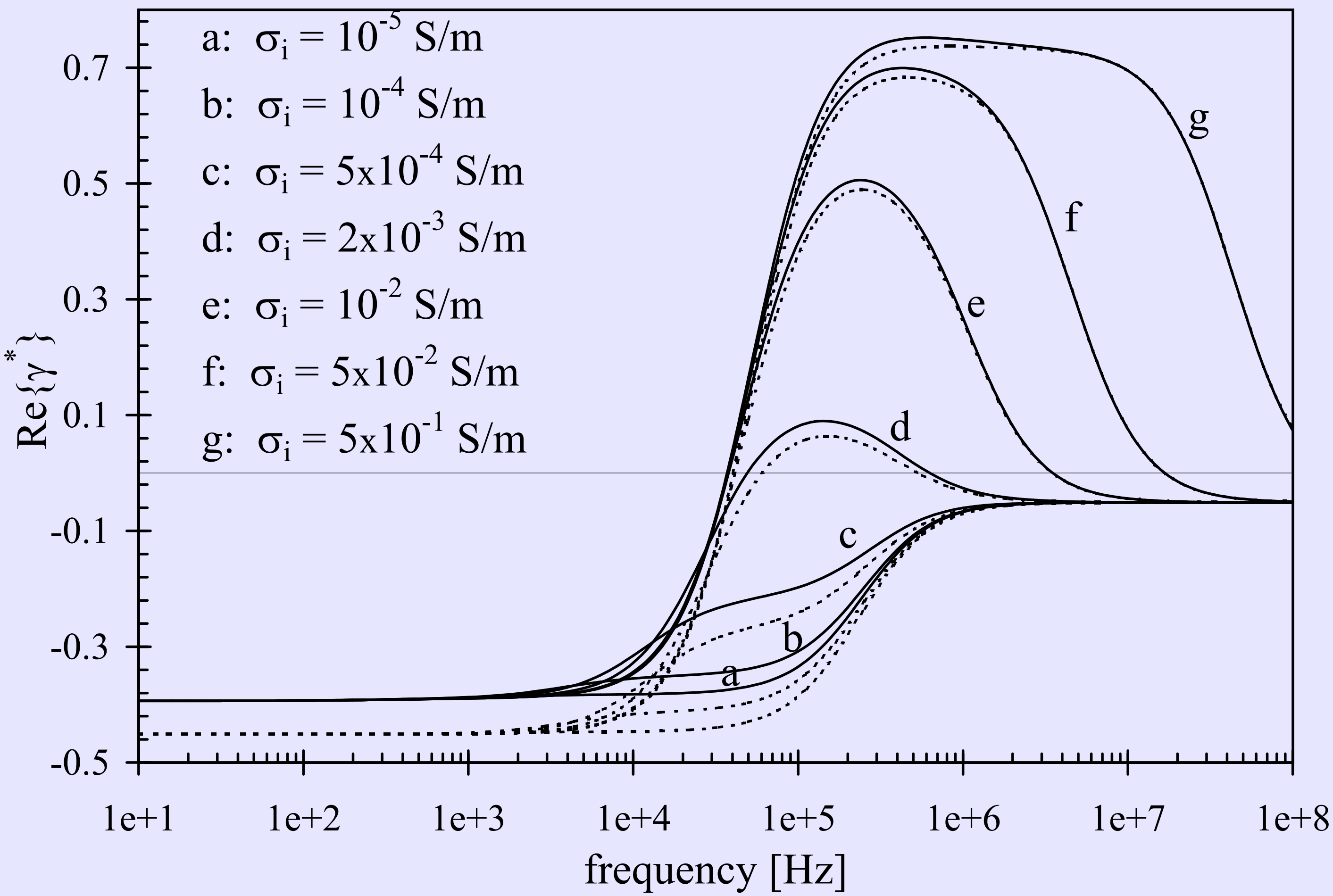

a: $\sigma_i = 10^{-5}$ S/m
b: $\sigma_i = 10^{-4}$ S/m
c: $\sigma_i = 5x10^{-4}$ S/m
d: $\sigma_i = 2x10^{-3}$ S/m
e: $\sigma_i = 10^{-2}$ S/m
f: $\sigma_i = 5x10^{-2}$ S/m
g: $\sigma_i = 5x10^{-1}$ S/m
Re{γ^*}
0.7
0.5
0.3
0.1
-0.1
-0.3
-0.5
1e+1
1e+2
1e+3
1e+4
1e+5
1e+6
1e+7
1e+8
frequency [Hz]
a
b
c
d
e
f
g

parameters used in the Figure

$R_a = 1.5\mu$m	$z_e^{\pm} = z_i^{\pm} = \pm 1$	$\rho^m = 10^3$ kg/m^3	$N_e = 300$
$\varepsilon_e = 78.36$	$D_e^{\pm} = D_w^{\pm} = D_i^{\pm} =$	$\rho^p = 1.2\times10^3$ kg/m^3	$N_w = 300$
$\varepsilon_m = 4$	2×10^{-9} m^2/s	$\eta = 8.904\times10^{-4}$ Pa s	$N_i = 200$
$\varepsilon_i = 70$	$z^f = -1$	$T = 298.4$ K	(number of
	$C^f = 3\times10^{23}$ 1/m^3	$R_a - R_b = 50$ nm	compartments)
$\kappa_e R_a = 48$	$\tilde{\zeta} = 1$	$R_b - R_c = 5$ nm	

Dielectric spectra

The permittivity (ε_{s}) of the dilute suspension is calculated using the dipole coefficient together with the Maxwell mixture formula:

$$\delta\varepsilon_{\mathrm{s}} = \varepsilon_{\mathrm{s}} - \varepsilon_{\mathrm{e}} = 3\nu\varepsilon_{\mathrm{e}}\left[\mathrm{Re}\left\{\gamma^*\right\} + \frac{\sigma_{\mathrm{e}}}{\omega\varepsilon_{\mathrm{o}}\varepsilon_{\mathrm{e}}}\mathrm{Im}\left\{\gamma^*\right\}\right]$$

❖ *Permittivity spectra for suspensions of cells:*

- *full lines: charged cells*
- *dashed lines: uncharged cells*
- *dotted curve: homogeneous particle with wall*

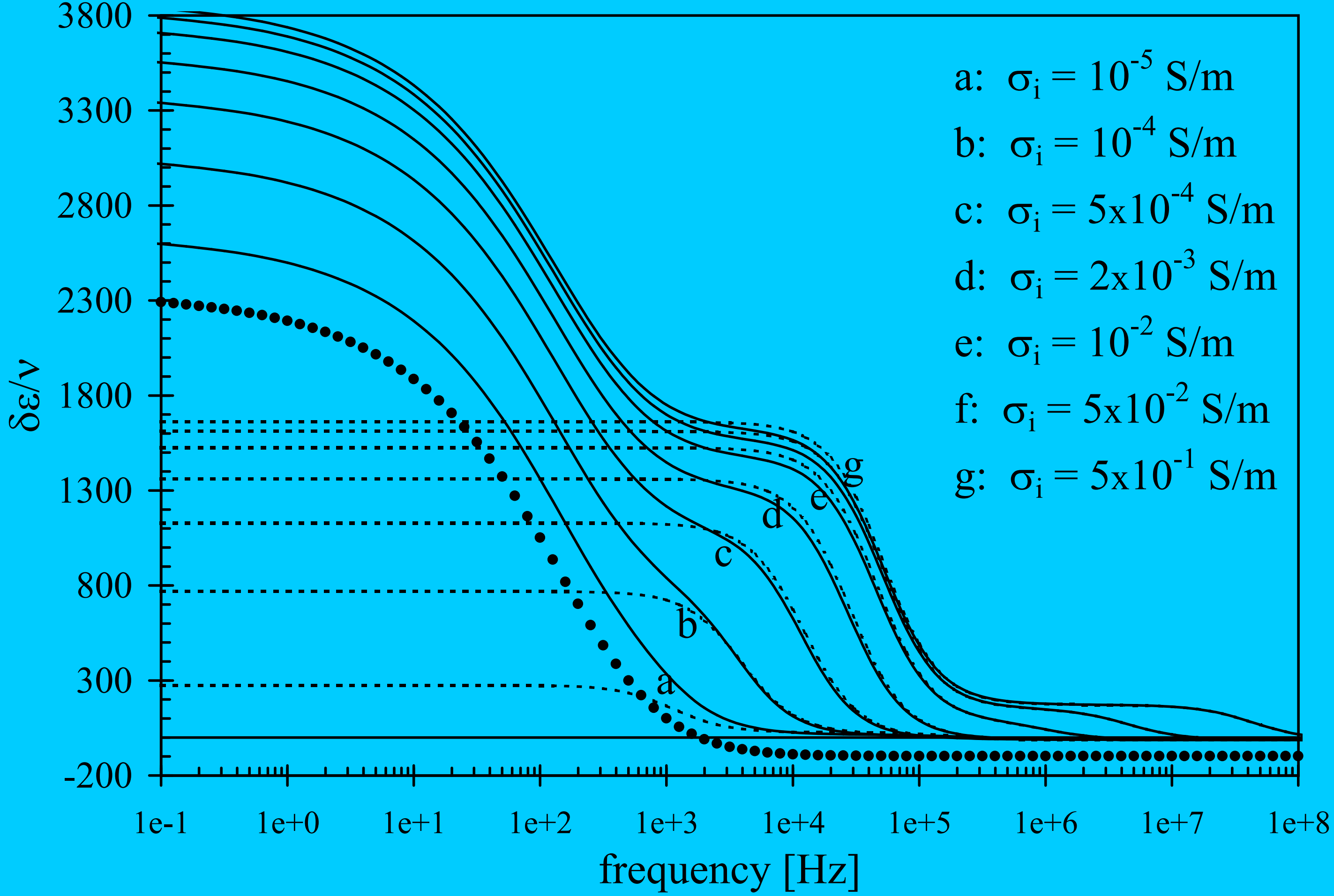

parameters used in the Figure (same as in the last figure)

$R_a = 1.5 \mu m$	$z_e^{\pm} = z_i^{\pm} = \pm 1$	$\rho^m = 10^3$ kg/m^3	$N_e = 300$
$\varepsilon_e = 78.36$	$D_e^{\pm} = D_w^{\pm} = D_i^{\pm} =$	$\rho^p = 1.2 \times 10^3$ kg/m^3	$N_w = 300$
$\varepsilon_m = 4$	2×10^{-9} m^2/s	$\eta = 8.904 \times 10^{-4}$ Pa s	$N_i = 200$
$\varepsilon_i = 70$	$z^f = -1$	$T = 298.4$ K	(number of
	$C^f = 3 \times 10^{23}$ 1/m^3	$R_a - R_b = 50$ nm	compartments)
$\kappa_e R_a = 48$	$\tilde{\zeta} = 1$	$R_b - R_c = 5$ nm	

- *spectra for charged and uncharged cells coincide at medium and high frequencies*
- *the low frequency limit changes due to the change in the* β*-dispersion amplitude*
- *the full spectra are obtained by adding the relaxations corresponding to each process (for sufficiently separated processes)*

❖ *Difference between the permittivity of a suspension of cells and a suspension of homogeneous particles surrounded by a wall divided by the permittivity of the cell suspension:*

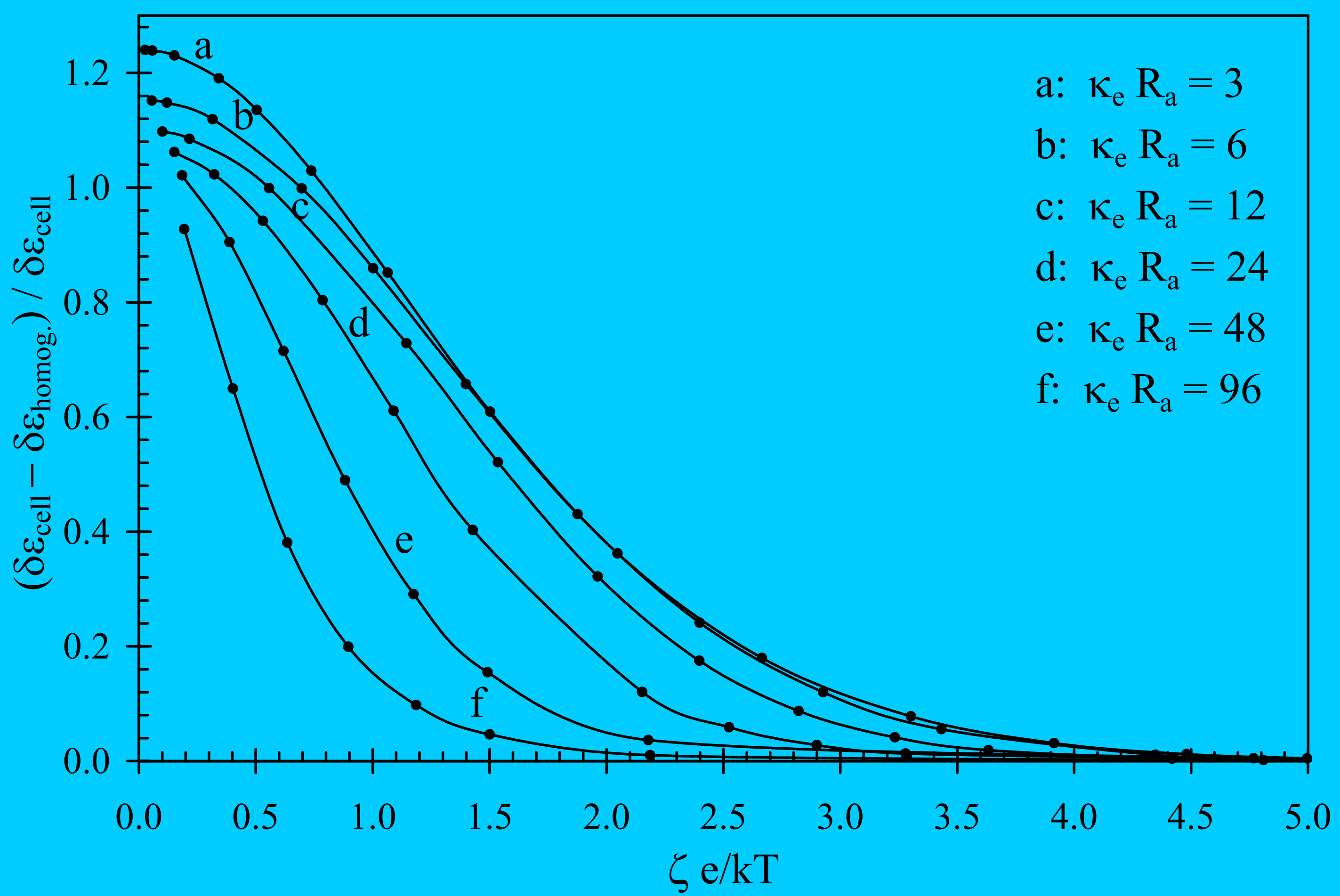

parameters used in the Figure (same as in the last figure)

$R_a = 1.5 \mu m$	$z_{\mathrm{e}}^{\pm} = z_{\mathrm{i}}^{\pm} = \pm 1$	$\rho^{\mathrm{m}} = 10^3$ kg/m^3	$N_{\mathrm{e}} = 300$
$\varepsilon_{\mathrm{e}} = 78.36$	$D_{\mathrm{e}}^{\pm} = D_{\mathrm{w}}^{\pm} = D_{\mathrm{i}}^{\pm} =$	$\rho^{\mathrm{p}} = 1.2 \times 10^3$ kg/m^3	$N_{\mathrm{w}} = 300$
$\varepsilon_{\mathrm{m}} = 4$	2×10^{-9} m^2/s	$\eta = 8.904 \times 10^{-4}$ $Pa\ s$	$N_{\mathrm{i}} = 200$
$\varepsilon_{\mathrm{i}} = 70$	$z^{\mathrm{f}} = -1$	$T = 298.4$ K	(number of
$\sigma_{\mathrm{i}} = 0.5$ S/m		$R_a - R_b = 50$ nm	compartments)
		$R_b - R_c = 5$ nm	

Electrorotation velocity

The electrorotation velocity (Ω) is calculated using the imaginary part of the dipole coefficient, together with the potential ($\delta\phi(r)$) and charge density ($\delta\rho(r)$) distributions (Zimmerman et al., 2002)

$$\Omega = \underbrace{-\frac{\varepsilon_0\,\varepsilon E_0}{2\eta R_a^3}\overbrace{\lim_{r\to\infty}\left[r^2\,\mathrm{Im}\{\delta\phi(r)+E_0 r\}\right]}^{\substack{\text{proportional to}\\ \mathrm{Im}\{\text{coef. dipolar}\}}}}_{\substack{\text{electrorotation velocity}\\ \text{classical term}}} - \underbrace{\frac{1}{3\eta}\int_{R_a}^{\infty}\left[1-\left(\frac{r}{R_a}\right)^3\right] g(r)\,dr}_{\substack{\text{electroosmotic term}\\ \text{(numerical integration)}}}$$

$$g(r) = \frac{1}{2r}\left[\mathrm{Re}\{\delta\rho(r)\}\,\mathrm{Im}\{\delta\phi(r)\} - \mathrm{Im}\{\delta\rho(r)\}\,\mathrm{Re}\{\delta\phi(r)\}\right]$$

❖ *Electrorotation spectra of cells*

∗ *full lines: numerical*

∗ *dashed lines: analytical (uncharged particles)*
(Zimmerman and Grosse, 2002)

- *constant fixed charge density* ($C^{\mathrm{f}} = 10^{24}$ *1/m*^{3}) $\Rightarrow$ *different* ζ*-potential for each curve*

- *numerical and analytical results comparison:*
  - ∗ δ: *excellent coincidence*
  - ∗ β: *very good coincidence for* $\kappa_{\mathrm{e}} R_a \gg 1$
  - ∗ α: *there are no analytical predictions for the system considered*

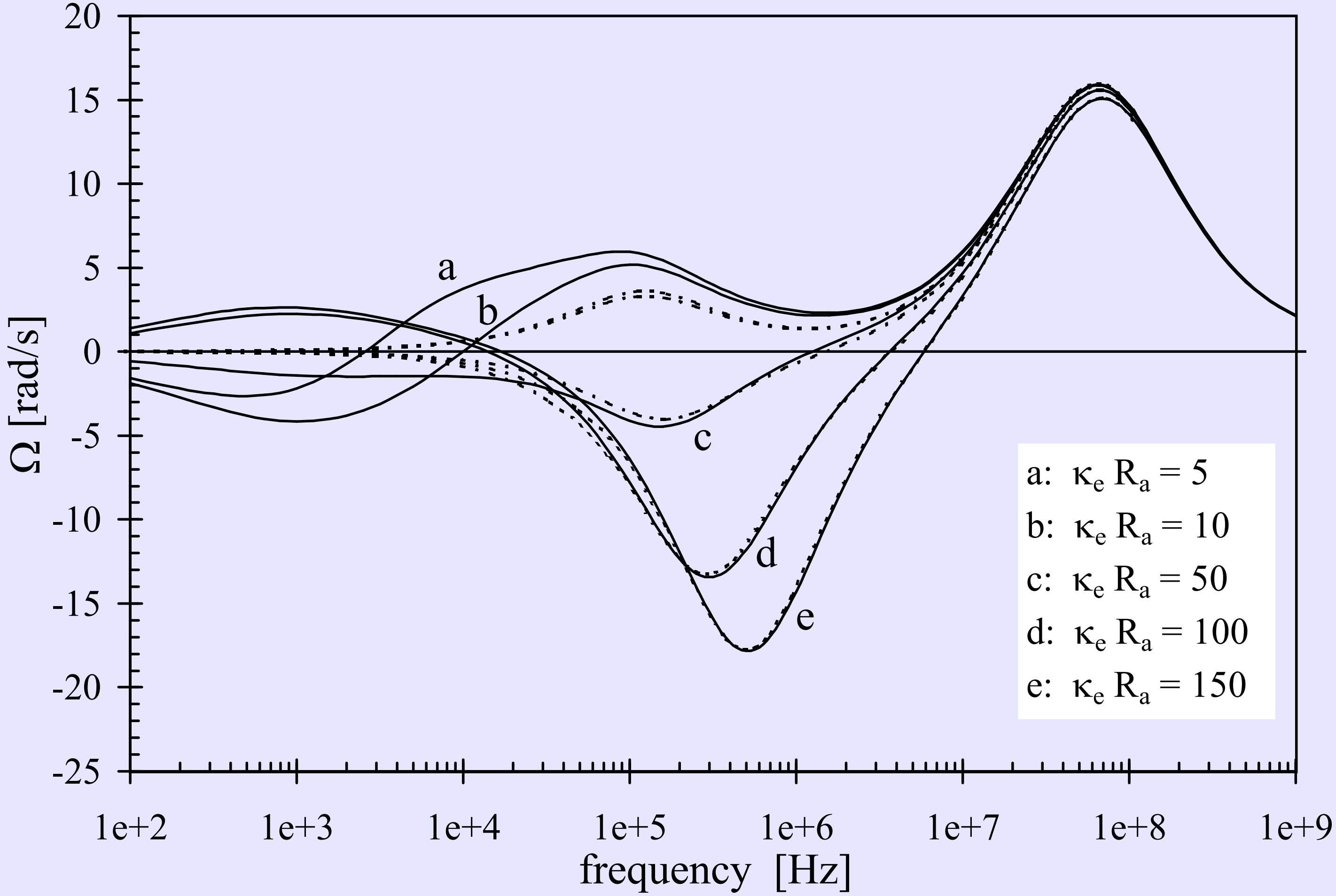

20
15
10
5
0
-5
-10
-15
-20
-25
Ω [rad/s]
1e+2
1e+3
1e+4
1e+5
1e+6
1e+7
1e+8
1e+9
frequency [Hz]
a
b
c
d
e
a: κe Ra = 5
b: κe Ra = 10
c: κe Ra = 50
d: κe Ra = 100
e: κe Ra = 150

parameters used in the Figure

$R_a = 1.5\mu m$	$\sigma_{\mathrm{i}} = 0.8\ S/m$	$\rho^{\mathrm{m}} = 10^3\ kg/m^3$
$R_a - R_b = 50\ nm$	$z_{\mathrm{e}}^{\pm} = z_{\mathrm{i}}^{\pm} = \pm 1$	$\rho^{\mathrm{p}} = 1.2 \times 10^3\ kg/m^3$
$R_b - R_c = 5\ nm$	$D_{\mathrm{e}}^{\pm} = D_{\mathrm{w}}^{\pm} = D_{\mathrm{i}}^{\pm} = 2 \times 10^{-9}\ m^2/s$	$\eta = 8.904 \times 10^{-4}\ Pa\ s$
$\varepsilon_{\mathrm{e}} = 78.36$	$z^{\mathrm{f}} = -1$	$E = 10000\ V/m$
$\varepsilon_{\mathrm{m}} = 4$	$\phi_{\mathrm{rf}} = 0$	$T = 298.4\ K$
$\varepsilon_{\mathrm{i}} = 70$		$N_{\mathrm{e}} = N_{\mathrm{w}} = 300$
		$N_{\mathrm{i}} = 200$

- *Electrorotation spectra of cells*
  - *full lines: numerical*
  - *dashed lines: analytical (uncharged particles)* (*Zimmerman and Grosse, 2002*)
  - *symbols: experimental data for* Cryptosporidium parvum *oocysts* (*Zimmerman, 2003*)

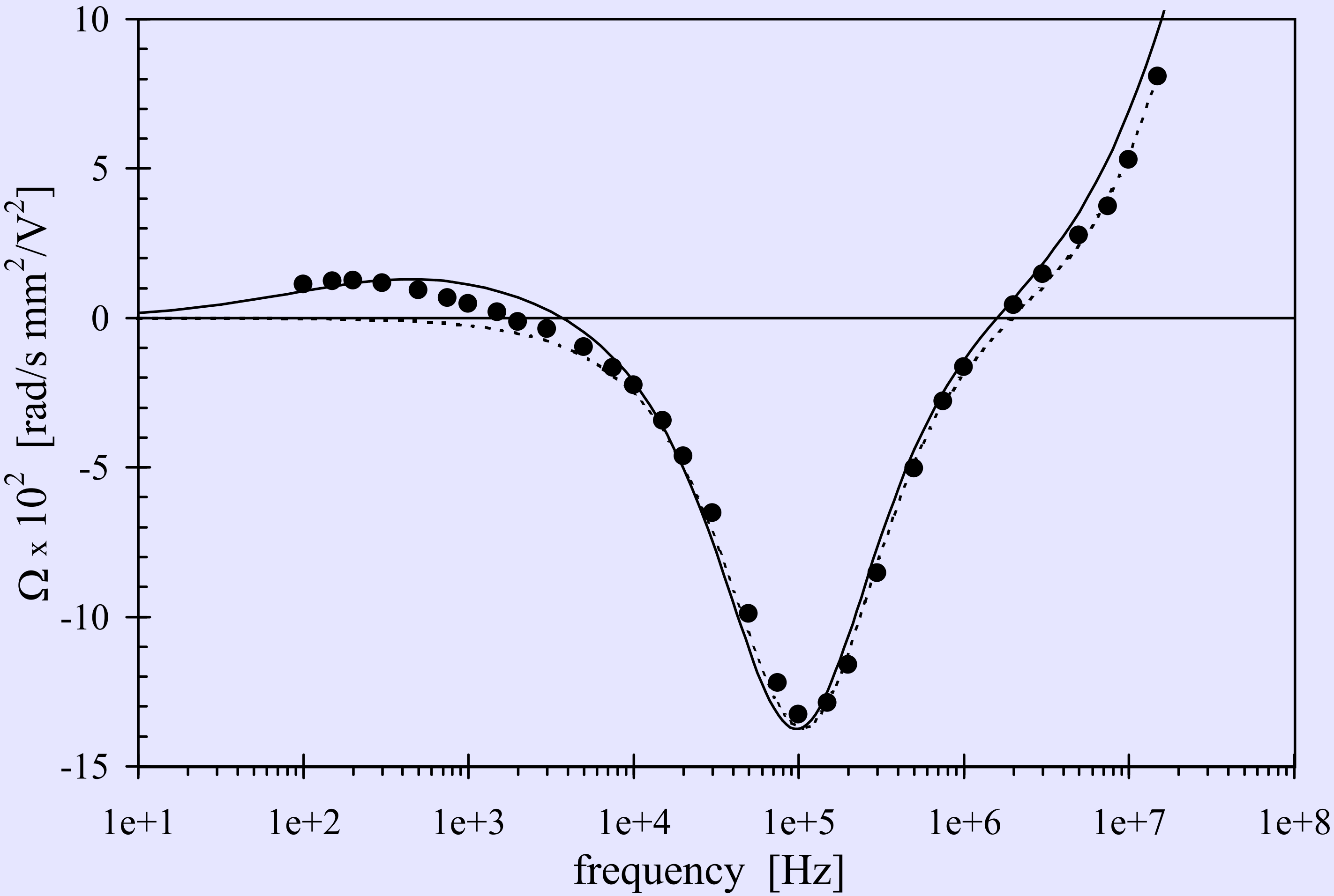

- *the system behaviour over the whole frequency range (including low frequencies) can be interpreted using the numerical electrorotation spectra* *parameters used in the Figure*

$R_a = 2.1\ \mu m$	$\sigma_e = 15.6\times 10^{-4}\ S/m$	$z^f = -1$
$R_a - R_b = 59.7\ nm$	$\sigma_i = 0.8\ S/m$	$C^f = 2\times 10^{24}\ 1/m^3$
$R_b - R_c = 7\ nm$	$z_e^{\pm} = z_i^{\pm} = \pm 1$	$\phi_{rf} = 0$
$\varepsilon_e = 78.36$	$D_e^- = D_w^- = D_i^{\pm} =$	$\rho^m = 10^3\ kg/m^3$
$\varepsilon_m = 3.9$	$2\times 10^{-9}\ m^2/s$	$\rho^p = 1.1\times 10^3\ kg/m^3$
$\varepsilon_i = 70$	$D_e^+ = 2.3\times 10^{-9}\ m^2/s$	$\eta = 8.9\times 10^{-4}\ Pa\ s$
$N_e = N_w = 300$	$D_w^+ = 5\times 10^{-9}\ m^2/s$	$T = 298.4\ K$
$N_i = 200$		

-

Born, M. (1920) Z. Physik *1:45–48.*

DeLacey, E. H., L. R.White (1981) J.Chem.Soc.Faraday Trans. *77(2):2007–2039.*

López-García, J. J., J.Horno, F.González-Caballero, C.Grosse, A. V.Delgado (2000) J. Colloid Interf. Sci. *228:95–104.*

López-García, J. J., J.Horno (2002) Study of electrokinetic phenomena in colloidal suspensions using the network simulation method. in J. H.Montijano, editor, Network Simulation Method *Capítulo 5, páginas 107–126. Research Signpost Kerala, India.*

Mangelsdorf, C. S., L. R.White (1992) J. Chem. Soc. Faraday Trans. *88(24):3567–3581.*

Mangelsdorf, C. S., L. R.White (1997) J. Chem. Soc. Faraday Trans. *93(17):3145–3154.*

O'Brien, R. W., L. R.White (1978) J. Chem. Soc. Faraday Trans. *74(2):1607–1626.*

Saville, D. (2000) J. Colloid Interf. Sci. *222:137–145.*

Zimmerman, V., C.Grosse, V. N.Shilov (2003) J. Phys. Chem. B *107(51):14612–14621.*

Zimmerman, V., C.Grosse (2002) Colloids Surf. A *197(1):69–77.*

Zimmerman, V., C.Grosse (2004) Numerical calculation of the dielectric spectra of cell-type particles. Sent for publication in J. Phys. Chem. B.

Zimmerman, V., V. N.Shilov, J. J.López-García, C.Grosse (2002) J. Phys. Chem. B *106(51):13384–13392.*

Zimmerman, V. (2003) Efectos No Lineales en Suspensiones Electrolíticas*. PhD thesis, Universidad Nacional de Tucumán, Argentina.*